Enzyme and Microbial Technology 52 (2013) 134–140

Contents lists available at SciVerse ScienceDirect

Enzyme and Microbial Technology

journal homepage: www.elsevier.com/locate/emt

Amperometric glucose biosensor based on glucose oxidase–lectin biospecific interaction

Juanjuan Zhang[a], Chengyan Wang[b], Shihong Chen[a,*], Dehua Yuan[a], Xia Zhong[a]

[a] Education Ministry Key Laboratory on Luminescence and Real-Time Analysis, College of Chemistry and Chemical Engineering, Southwest University, Chongqing 400715, China
[b] Fuling Senior High School, Chongqing 408100, China

ARTICLE INFO

Article history:
Received 2 March 2012
Received in revised form
13 December 2012
Accepted 16 December 2012

Keywords:
Gold/platinum hybrid
Zinc oxide nanorods
Concanavalin A
Glucose oxidase
Glucose
Biosensor

ABSTRACT

An amperometric glucose biosensor based on high electrocatalytic activity of gold/platinum hybrid functionalized zinc oxide nanorods (Pt–Au@ZnONRs) and glucose oxidase (GOx)–lectin biospecific interaction was proposed. The Pt–Au@ZnONRs, which were prepared through a multiple-step chemosynthesis, were modified onto the surface of glassy carbon electrode (GCE) by a simple casting method due to the excellent film forming ability of the Pt–Au@ZnONRs suspension. Subsequently, a layer of porous gold nanocrystals (pAu) film was assembled onto the Pt–Au@ZnONRs film by immersing the electrode in $HAuCl_4$ solution to perform the electrochemical deposition at a constant potential of −0.2 V. Following that, Concanavalin A (ConA) was immobilized onto the surface of pAu film through physical adsorption and covalent binding interactions between gold nanomaterials and the amino groups or thiol groups of ConA protein. Finally, the GOx was easily immobilized on the ConA/pAu/Pt–Au@ZnONRs/GCE by the biospecific interaction between GOx and ConA. The Pt–Au@ZnONRs composites were characterized using transmission electron microscopy (TEM) and X-ray photoelectron spectroscopy (XPS). Cyclic voltammetry (CV) was used to characterize the assembly process of the modified electrode. Proposed biosensor showed a high electrocatalytic activity to the glucose with a wide linear range covering from 1.8 μM to 5.15 mM, a low detection limit of 0.6 μM and a low apparent Michaelis–Menten constant (K_M^{app}) of 0.41 mM. Furthermore, the biosensor exhibited good reproducibility and long-term stability, as well as high selectivity. The integration of Pt–Au@ZnONRs and GOx–lectin biospecific interaction would offer potential promise for the fabrication of biosensors and biocatalysts.

1. Introduction

Since the pioneering work of Clark and Lyons, there has been an ever growing interest in the design of enzyme electrodes as they are faster and more economical tools for application in hospital, clinical, chemical and pharmaceutical laboratories [1,2]. The performance of an enzyme electrode, including lifetime, linear range, sensitivity, selectivity, response time, stability and susceptibility to interfering agents, depends on the method used for the immobilization of the enzyme [3]. Therefore, the method used for the efficient immobilization of the biomolecule/enzyme is a key factor that must be taken into consideration in developing a biosensor. Various approaches including adsorption [4], cross-linking [5], covalent binding [6] and entrapment [7–9] have been widely employed. In these traditional immobilization techniques, the biomolecule/enzyme was randomly immobilized on the surface of the modified electrode. One of the key difficulties with immobilization using such methods is that it results in a multipoint attachment of the enzyme to the surface thereby limiting its mobility, potentially resulting in steric hindrance of biological interactions and also potential denaturation of the biomolecules [10,11].

The oriented and site-specific immobilization of enzymes can overcome above difficulties involved in random immobilization of enzyme and has become crucial for the rational design of biosensors. It can be achieved through the biospecific interactions, including sugar–lectin, avidin–biotin, sugars–histidine, and metal chelates–cysteine [12]. The sugar recognition and binding properties of lectins, such as ConA, has attracted much attention as many biomolecules, including enzymes, are glycosylated. ConA is a plant lectin that is capable of binding to sugars such as mannose and glucose. The protein is a tetramer made up of four identical subunits with each subunit presenting a single carbohydrate domain [13]. The lectin is known to bind tightly to the tri-mannose core structure of N-linked glycans. GOx, which is often produced via expression in Yeast, displays such N-linked glycan structures and so ConA can be utilized to immobilize GOx via specific interaction with these glycans. Kobayashi and Anzai [14] employed ConA to

* Corresponding author. Tel.: +86 23 68253172; fax: +86 23 68253172.
E-mail address: cshong@swu.edu.cn (S. Chen).

0141-0229/$ – see front matter © 2012 Elsevier Inc. All rights reserved.
http://dx.doi.org/10.1016/j.enzmictec.2012.12.005

assemble horseradish peroxidase (HRP) and GOx into multilayer films and achieved a biosensor for the determination of hydrogen peroxide and glucose. Li et al. [15] constructed a biosensor based on Pt nanoparticles supported on carbon nanotubes and the biospecific affinity of ConA and glucose oxidase. The resulting biosensor exhibited a good biocatalytic activity toward glucose.

Zinc oxide nanomaterials (nano-ZnO) have been the target of numerous investigations due to their unique properties, including high surface-to-volume ratio, non-toxicity, chemical stability, electrochemical activity, and favorable electron-communication features [16]. Furthermore, the high isoelectric point (IP: 9.5) of nano-ZnO makes it suitable for the absorption of GOx with low IP of 4.2 [17,18]. With the wide application of nano-ZnO, various noble metals–ZnO composites, such as Pt-incorporated fullerene-like ZnO nanospheres [19], AgNPs–ZnO composites [20] and ZnO-Au nanocomposites [21], have been prepared and aroused much interest in electroanalytical chemistry field.

Based on above observation, in this work, gold/platinum hybrid functionalized zinc oxide nanorods (Pt–Au@ZnONRs) were prepared through one-step reduction of 'H_2PtCl_6 growth solution' and selective deposition of Pt on the ZnONRs surface. Herein, gold nanoparticles seeds (3–4 nm) acted as the crystal cores for the growth of Pt, leading to the formation of gold/platinum hybrid on the ZnONRs surface. Next, on the Pt–Au@ZnONRs modified electrode, the porous gold nanocrystals (pAu) were deposited by electrochemical reduction of gold chloride tetrahydrate (HAuCl4) solution for the immobilization of ConA since gold nanomaterial is an excellent candidate for the immobilization of ConA [22–24]. Finally, based on site-specific interactions between GOx and ConA, GOx was efficiently immobilized onto the surface of pAu/Pt–Au@ZnONRs. The performance and the experimental parameters for the determination of glucose were investigated at the proposed biosensor. Due to the integration of the unique electrocatalytic activity of Pt–Au@ZnONRs composite and the sugar–lectin based biospecific immobilization for the enzyme, this glucose biosensor exhibits enhanced performance compared to other previously reported sensors [25–31]. This construction strategy would offer potential promise for the fabrication of biosensors and biocatalysts.

2. Experimental

2.1. Chemical

Glucose oxidase, $HAuCl_4{\cdot}4H_2O$, $H_2PtCl_6{\cdot}6H_2O$ (99.9%) and concanavalin A (from Canaalia ensiformis, jack bean) were purchased from Sigma–Aldrich (Shanghai) Trading Co., Ltd. Tetraethoxysilane (TEOS), 3-aminopropyltriethoxysilane (APTES) and trioctylamine were supplied by Chemical Reagent Co., Shanghai, China. Cetyltrimethylammonium bromide (CTAB), Zinc acetate, cobalt (II) acetate, ethanol, ammonia solution, sodium citrate, L-cysteine, ascorbic acid and uric acid were obtained from Chemical Regent Co. Chongqing, China. Gold nanoparticles seeds (3–4 nm) solution was prepared according to the literature [32]. Briefly, 0.60 mL of ice-cold 0.010 M $NaBH_4$ was added into the mixture of CTAB solution (5 mL, 0.20 M) and 5.0 mL of 0.00050 M $HAuCl_4$ under stirred condition. The resulted brownish yellow solution was vigorously stirred continued for 2 min to obtain the nanogold seeds solution. Phosphate buffer saline (PBS) with various pH values was prepared with stock standard solutions of Na_2HPO_4 and KH_2PO_4. The supporting electrolyte was 0.1 M KCl. Deionized water was used throughout the experiments. GOx solution (2 mg mL^{-1}) was prepared with 0.1 M pH 7.0 PBS.

2.2. Apparatus and measurements

Transmission electron microscopy (TEM) was investigated using a TECNAI 10 (PHILIPS FEI Co., The Netherlands). X-ray photoelectron spectroscopy (XPS) measurements were performed on a VG Scientific ESCALAB 250 spectrometer, using Al KR X-ray (1486.6 eV) as the light source. The electrochemical experiments were performed at room temperature utilizing an electrochemical workstation (CHI660D) with a conventional three-electrode system. A bare or modified glassy carbon electrode (GCE, 4 mm in diameter) was used as the working electrode, with saturated calomel electrode (SCE) as the reference electrode, and platinum as the counter electrode.

2.3. Preparation of Pt–Au@ZnONRs

2.3.1. Synthesis of ZnONRs

In a typical synthesis, zinc acetate (0.2335 g) and cobalt acetate (0.01295 g) were added into trioctylamine (10 mL) in a round-bottomed flask equipped with a condenser. The mixture was rapidly heated to 300 °C. The solids were dissolved slowly under constant stirring. The color of the solution turned green after heated for 15–20 min, indicating the start of nanorods formation. The reaction was continued for 120 min and then cooled down to room temperature. The green zinc oxide nanorods (ZnONRs) was collected through centrifugation and washed several times with ethanol to remove cobalt precursor and cobalt metal particles.

2.3.2. Synthesis of amino-functionalized ZnONRs

ZnONRs were functionalized with amino as following: in the mixture of 2-propanol (10 mL) and ethanol (20 mL), 15 mg ZnONRs was dispersed to give a suspension of 0.5 mg mL^{-1}. Subsequently, 2.5 mL deionized water and 0.8 mL ammonia solution (25%) were added into the suspension, followed by the addition of 25 μL APTES and 50 μL TEOS under continuous stirring. The mixture was continually stirred for 8 h at room temperature. The resulting amino functionalized ZnONRs were collected through centrifugation and washed with ethanol several times. The final product was dried in vacuum.

2.3.3. Synthesis of Pt–Au@ZnONRs

Firstly, the amino functionalized ZnONRs (15 mg) was dispersed in ethanol (5 mL). Then, 50 mL of freshly prepared gold seed solution was added into above suspension under stirring. The mixture was stirred for 5 h to prepare gold nanoparticles supported ZnONRs. The precipitate was collected by centrifugation and washed 3 times with water, and then re-dispersed in 50 mL water for further use. When the dispersion of gold nanoparticles supported ZnONRs was heated to boiling, 2 mL of 1% H_2PtCl_6 and 3 mL of 1% sodium citrate were added, followed by the addition of 5 mL ascorbic acid. Herein, ascorbic acid served as a reductant for the reduction of H_2PtCl_6. The reaction was allowed to continue for 30 min to achieve Pt–Au hybrid functionalized ZnO nanorods (Pt–Au@ZnONRs), which was collected through centrifugation and washed with water several times. The final product was dried in vacuum.

2.4. Preparation of glucose biosensor

The GCE was carefully polished with alumina slurry (grain size, 0.3 μm and 0.05 μm) until a mirror was obtained. Ultrasonic rinsing with ethanol and water was necessary to remove the alumina residues from the electrode surface. Pt–Au@ZnONRs suspension (2.0 mg mL^{-1}) was prepared by dispersing 4 mg of Pt–Au@ZnONRs into 2 mL ethanol with the aid of ultrasonic agitation. Pt–Au@ZnONRs suspension (8 μL) was dropped onto the cleaned GCE surface and dried in the air. The excellent film forming ability of the Pt–Au@ZnONRs suspension made the Pt–Au@ZnONRs modified electrode easy preparation. Then, the Pt–Au@ZnONRs/GCE was immersed in 2 mL of 1% $HAuCl_4$ solution and the electrochemical deposition was performed at a constant potential of −0.2 V for 30 s, resulting in the formation of a layer of porous gold nanocrystals (pAu) film on the modified electrode. After cleaned with water, the electrode was incubated in a ConA solution (0.3 mg mL^{-1} in pH 7.0 PBS containing 1 mmol L^{-1} $CaCl_2$ and 1 mmol L^{-1} $MnCl_2$) for 5 h. In this case, the immobilization of ConA may be due to the following facts. On the one hand, gold nanomaterials with large surface area and high-surface free energy can physically adsorb ConA. On the other hand, strong binding interactions between gold nanomaterials and the amino groups or thiol groups of ConA protein can achieve the covalent immobilization of ConA. Finally, the modified electrode was immersed in GOx solution (2 mg mL^{-1}) for 10 h to assemble the GOx layer through biospecific ConA–sugar interaction. The resulted electrode (GOx/ConA/pAu/Pt–Au@ZnONRs/GCE) was stored at 4 °C in a refrigerator when not in use. The procedure for constructing the modified electrode was schematically shown in Scheme 1. The GOx/pAu/Pt–Au@ZnONRs/GCE was fabricated using the same procedure described above for GOx/ConA/pAu/Pt–Au@ZnONRs/GCE except that ConA was not involved.

3. Results and discussion

3.1. Characterization of Pt–Au@ZnONRs

Transmission electron microscopy (TEM) was used to investigate the topographies of ZnONRs and Pt–Au@ZnONRs, respectively, and the results were shown in Fig. 1. From the TEM images of ZnONRs (Fig. 1A), it was seen that ZnONRs presented straight and smooth rod-shaped structures, with an average diameter of 18 nm and the length ranging from 50 nm up to 300 nm. Through one-step reduction of 'H_2PtCl_6 growth solution' and selective deposition of Pt on the ZnONRs surface driven by the Au seeds acting as nucleation centers, Pt shell was grown around the Au seeds particles leading

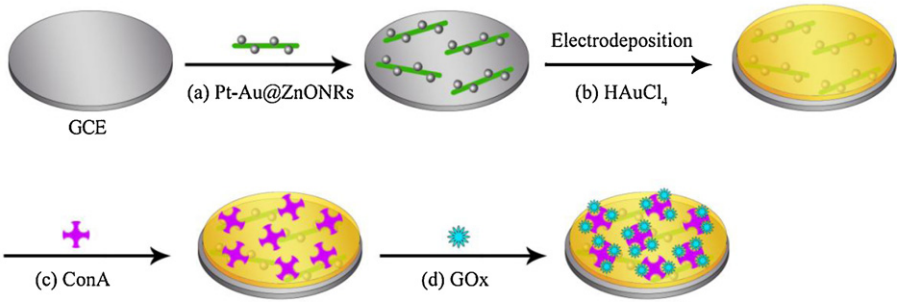

Scheme 1. The illustration of the preparation process of GOx/ConA/pAu/Pt–Au@ZnONRs/GCE.

to the formation of the gold–platinum hybrid modified ZnONRs. The TEM images of Pt–Au@ZnONRs were shown in Fig. 1B. As expected, a layer shell structure composed of gold-platinum hybrid nanoparticles was clearly observed at the surface of ZnONRs and the diameter of Pt–Au@ZnONRs is about twice as large as that of ZnONRs.

In order to further confirm the chemical composition of Pt–Au@ZnONRs nanocomposite, X-ray photoelectron spectroscopy (XPS) measurements were done and the XPS spectra of O1s, Zn2p, Au4f and Pt4f were shown in Fig. 2A–D, respectively. As seen from Fig. 2A, the O1s spectrum was fitted with O1s spectrum of ZnO. The Zn2p spectrum in Fig. 2B showed a doublet with binding energies of 1021.1 and 1044.9 eV, which can be identified as $Zn2p_{3/2}$ and $Zn2p_{1/2}$ lines, respectively. As expected, Au4f doublet features with binding energies of 83.6 eV for $4f_{7/2}$ and 87.6 eV for $4f_{5/2}$, and Pt4f doublet features with binding energies of 70.8 eV for $4f_{7/2}$ and 74.1 eV for $4f_{5/2}$ can be clearly observed at the Pt–Au@ZnONRs nanocomposite, suggesting the formation of Pt–Au hybrid on the surface of ZnONRs and the successful preparation of Pt–Au@ZnONRs nanocomposite.

3.2. Electrochemical characteristics of the fabricated biosensor

Cyclic voltammetry (CV) was used to characterize the assembly process of the modified electrode and the corresponding cyclic voltammograms (CVs) in $[Fe(CN)_6]^{3-}/[Fe(CN)_6]^{4-}$ solution were shown in Fig. 3. The CVs of bare GCE presented a pair of well-defined redox peaks (curve a), which is attributed to the redox behavior of $[Fe(CN)_6]^{3-}/[Fe(CN)_6]^{4-}$. An obvious increase in reduction and oxidation peak current was observed after Pt–Au@ZnONRs were deposited on the electrode (curve b), implying that Pt–Au@ZnONRs possesses good conductivity and can facilitate the electron transfer. A further increase of the peak currents was obtained after the pAu film was deposited on the Pt–Au@ZnONRs-modified electrode (curve c), indicating that the pAu can act as tiny conduction centers to facilitate the electron transfer at the electrode surface. The successful assembly of ConA and GOx on the electrode surface prevents the penetration of the conducting ions. This was proved by a significant reduction in the voltammetric response of the electrode, as shown in curve d and curve e, respectively.

3.3. Optimization of the experimental conditions

To obtain an optimal response for glucose, the influence of pH, applied potential and the deposition time of pAu film on the response of the biosensor was investigated. The effect of pH was tested in a series of 0.1 M PBS with pH from 5.0 to 8.5 under constant glucose concentration of 1.5 mM. The change of chronoamperometric current with the pH was shown in Fig. 4A. As can be seen, the maximum response appeared at pH 7.0. Thus all experiments have been conducted in pH 7.0 PBS.

Fig. 4B showed the dependence of the chronoamperometric current response to 1.5 mM glucose on the applied potential in the range from 0.2 to 0.6 V. As observed, when the applied potential increased from 0.2 to 0.6 V, the response currents of the biosensor would accordingly increase. However, an applied potential of

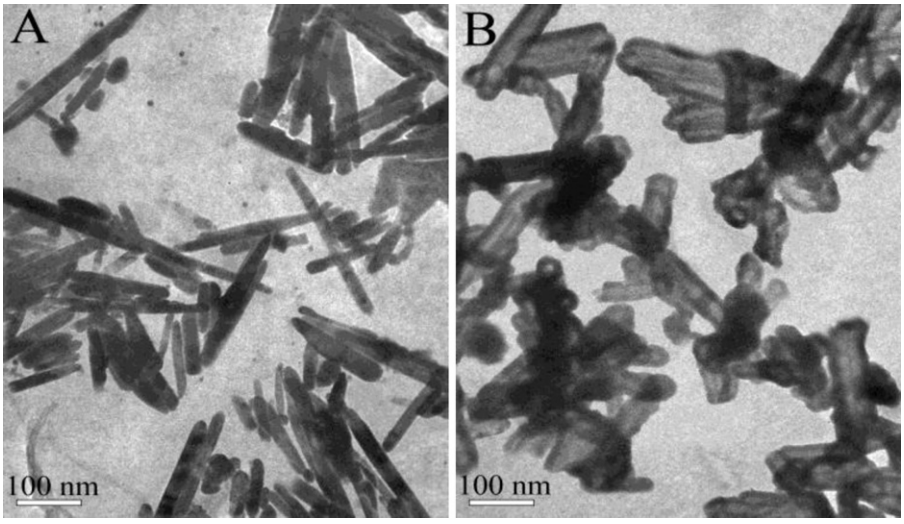

Fig. 1. TEM images of (A) ZnO nanorods and (B) Pt–Au@ZnONRs.

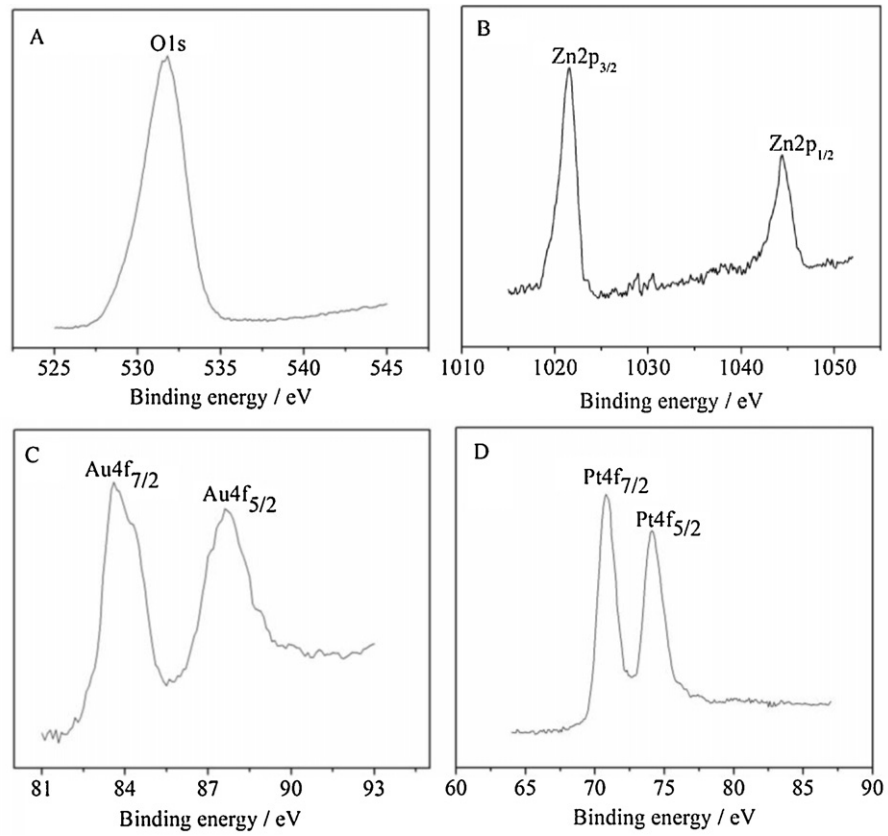

Fig. 2. XPS spectra of the Pt–Au@ZnONRs: (A) O1s, (B) Zn2p, (C) Au4f and (D) Pt4f.

0.45 V was selected for the amperometric determination of glucose. Because not only sufficient current responses could be obtained but also the risk for interfering reactions of other electroactive species in the solution could be minimized at an applied potential of 0.45 V.

The effect of deposition time of pAu film on the response of the biosensor was also investigated from 20 s to 100 s, and the result was shown in Fig. 4C. It can be seen that the chronoamperometric current increased sharply from 20 s to 60 s, and reached the maximum at 60 s. The further increase of deposition time seemed to decrease the response current. The reason was that the deposition of excessive Au nanoparticles resulted in the decrease of the real surface area of the electrode. Therefore, the optimum deposition time of pAu film is 60 s.

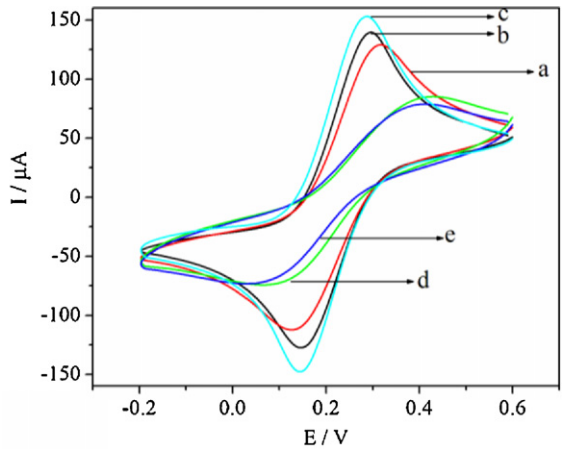

Fig. 3. CVs of (a) bare GCE, (b) Pt–Au@ZnONRs/GCE, (c) pAu/Pt–Au@ZnONRs/GCE, (d) ConA/p/Pt–Au@ZnONRs/GCE and (e) GOx/ConA/pAu/Pt–Au@ZnONRs/GCE in 5.0 mM $K_3[Fe(CN)_6]/K_4[Fe(CN)_6]$ (1:1). Scan rate: 50 mV s^{-1}.

3.4. Cyclic voltammetric response of the biosensor to glucose

The catalytic activity of the biosensor toward glucose was investigated by CV. Fig. 5 displayed the CVs of the biosensor in PBS in the absence (curve a) and in the presence of 5.0 mM glucose (curve b). With the addition of glucose, the biosensor triggers bioelectrocatalytic reaction, which dramatically changes the CVs with a sharp increase of the oxidation current, indicating the enzyme biosensor exhibited excellent electrocatalytic activity toward glucose. The reactions can be described as follows:

$$\beta\text{-D-glucose} + O_2 \xrightarrow{GOx} \beta\text{-D-gluconolactone} + H_2O_2 \quad (1)$$

$$2H_2O_2 \xrightarrow{E} 2H_2O + O_2 + 2e^- \quad (2)$$

In the PBS, glucose is oxidized by the dissolved oxygen with the aid of the immobilized GOx and H_2O_2 is liberated during the course. The generated H_2O_2 is subsequently oxidized at the biosensor and gives rise to the anodic current. The glucose concentration can be determined by measuring the current derived from the electrochemical reaction of H_2O_2.

3.5. Amperometric response of the biosensor to glucose

Fig. 6A depicted the current–time curves for GOx/ConA/pAu/Pt–Au@ZnONRs/GCE (curve a) and GOx/pAu/Pt–Au@ZnONRs/GCE (curve b) upon the successive addition of different concentrations of glucose in a stirred PBS under the optimal experiment conditions. Both the glucose biosensors exhibited rapid responses to the each addition of glucose, and the response time was less than 5 s (reaching 95% of stabilized

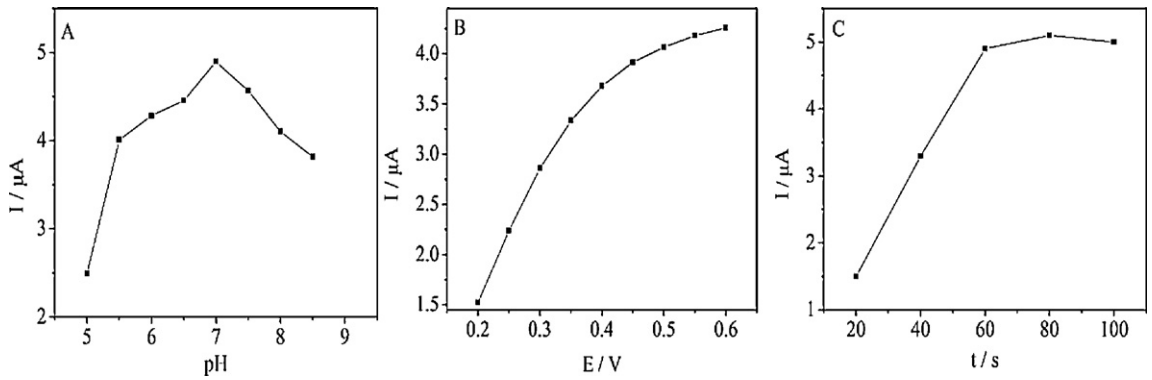

Fig. 4. Dependence of the current response of the biosensor to 1.5 mM glucose on (A) pH of PBS at an applied potential of 0.45 V, (B) on the applied potential in 0.1 M PBS (pH 7.0) and (C) on the deposition time of pAu film.

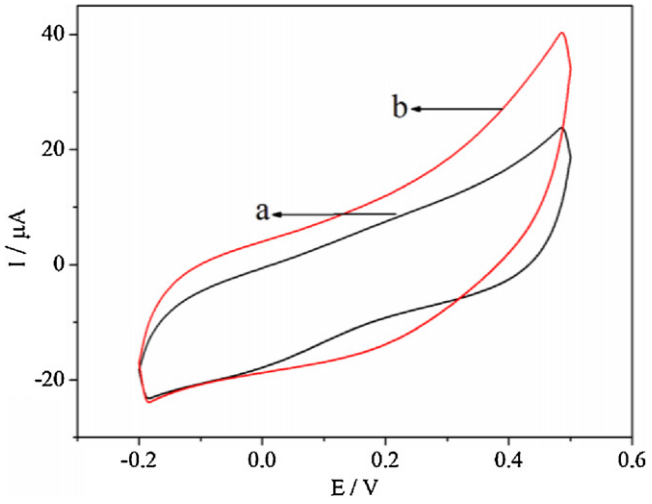

Fig. 5. CVs of the biosensor in 0.1 M PBS (pH 7.0) without glucose (a) and with 5.0 mM glucose (b). Scan rate: 50 mV s^{-1}.

current signal). But the GOx/ConA/pAu/Pt–Au@ZnONRs/GCE displayed much larger amperometric response than the GOx/pAu/Pt–Au@ZnONRs/GCE with respect to the same amount of glucose. The calibration curves for both biosensors were shown in Fig. 6B. The linear range of GOx/ConA/pAu/Pt–Au@ZnONRs/GCE (curve a) for glucose was 1.8 μM ~5.15 mM, which was wider than that of GOx/pAu/Pt–Au@ZnONRs/GCE (6 μM–5.15 mM, curve b). A higher sensitivity of 3.26 μA/mM was obtained for the GOx/ConA/pAu/Pt–Au@ZnONRs/GCE and it was around 3-fold greater than that of GOx/pAu/Pt–Au@ZnONRs/GCE (1.12 μA/mM). The detection limits, based on the signal to noise ratio of 3, was estimated to be 2.0 μM for GOx/pAu/Pt–Au@ZnONRs/GCE, while the value for GOx/ConA/pAu/Pt–Au@ZnONRs/GCE was only 0.6 μM. This was due to the property of the ConA, which could achieve the oriented and site-specific immobilization of enzymes.

The apparent Michaelis–Menten constant (K_M^{app}), which gives an indication of the enzyme–substrate kinetics, can be calculated according to the Lineweaver–Burk equation [33]:

$$\frac{1}{I_{SS}} = \frac{1}{I_{max}} + \frac{K_M^{app}}{I_{max}C}$$

Here, I_{SS} is the steady-state current after the addition of substrate and I_{max} is the maximum current under saturated substrate condition. Both I_{SS} and I_{max} can be obtained from amperometric experiments. C is the bulk concentrate of the substrate. According to the slope (K_M^{app}/I_{max}) and the intercept ($1/I_{max}$) for the plot of the reciprocals of the steady-state current (I_{SS}) versus the reciprocals of the concentration (C) of glucose, the value of K_M^{app} for the GOx/ConA/pAu/Pt–Au@ZnONRs/GCE is estimated to be 0.41 mM. The low value of K_M^{app} indicates that GOx immobilized through GOx–ConA biospecific interaction could well retains its bioactivity and has a high biological affinity to glucose.

In addition, the analytical performance of the developed biosensor has been compared with those of other glucose biosensors reported in the literatures [25–31]. As can be seen from Table 1, for the proposed biosensor, the linear range was wider than those in most of works, the detection limit was lower, and the value of K_M^{app} was also lower. The reasons might be ascribed to the following facts. On the one hand, the good biocompatibility of pAu film and the good catalytic activity of Pt–Au@ZnONRs were integrated together, which could be favorable for maintaining the biological activity and improving the response sensitivity for the

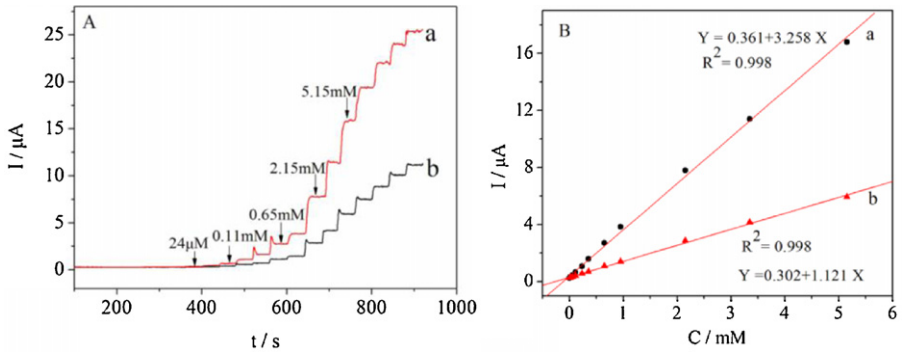

Fig. 6. (A) Typical current–time response curves for successive addition of glucose at (a) GOx/ConA/pAu/Pt–Au@ZnONRs/GCE and (b) GOx/pAu/Pt–Au@ZnONRs/GCE in stirring 0.1 M PBS at an applied potential of 0.45 V. (B) The corresponding calibration curves.

Table 1
Comparison of the performance of different glucose biosensors.

Biosensor fabrication	Detection potential	Linearity range	Detection limit	Sensitivity	K_m	Ref.
GOx/Au/CS–IL–MWNT(SH)/ITO	0.10 V (vs. Ag/AgCl)	1–10 mM	10 μM	4.10 μA mM^{-1}	–	[25]
(PAH–MCNT/HRP)n/(ConA/GOD)n/Au	−0.15 V	$2.0 \times 10^{-3}$to 1.7×10^{-1} mM	0.25 μM	–	–	[26]
CHIT/GOx/NiO/GCE	0.35 V	1.5–7 mM	47 μM	4.3 μA mM^{-1}	7.76 mM	[27]
GOD/Pt/OMC/Au	−0.15 V	0.05–3.70 mM	0.05 mM	0.38 μA mM^{-1}	–	[28]
GOD/GNp/CS/GOD/GNp/PAA/Pt	0.6 V (vs. Ag/AgCl)	0.5–16 mM	7.0 μM	0.555 μA mM^{-1}	10.5 mM	[29]
PB/MWNTs-GOx-CS-ICPTES/GCE	−0.1 V	2.5×10^{-2} to 1.3 mM	7.5 μM	15.2 μA mM^{-1} cm^{-2}	3.67 mM	[30]
Nafion/GOD/C–ZnO/Ti	−0.45 V	1.0×10^{-2} to 1.6 mM	2.0 μM	35.3 μA mM^{-1} cm^{-2}	~1.54 mM	[31]
GOD/ConA/Nano-Au/Pt–Au@ZnONRs/GCE	0.45 V	1.8×10^{-3} to 5.15 mM	0.6 μM	3.26 μA mM^{-1}	0.41 mM	This work

electrocatalytic oxidation of glucose at the biosensor. On the other hand, the matrix could achieve the oriented and site-specific immobilization of GOx in the presence of ConA, which could improve the affinity to glucose.

3.6. The reproducibility and stability of the biosensor

The operational reproducibility of the enzyme electrode was examined by measuring the responses to 0.5 mM glucose. RSD for ten successive measurements with the same biosensor was 2.5%. The reproducibility of the construction of the biosensors was evaluated at six modified electrodes separately fabricated under the same conditions. The results revealed that the biosensors had acceptable reproducibility with a RSD of 5.7%. The stability of the biosensor was evaluated by measuring the amperometric response to 0.5 mM glucose. When not in use, the biosensor was suspended over 0.1 M PBS (pH 7.0, containing 1 mmol L^{-1} $CaCl_2$ and 1 mmol L^{-1} $MnCl_2$) at 4 °C in a refrigerator and measured at intervals of one day, the biosensor retained 92.3% of its original response current after one week. After 3 weeks, the current response of the biosensor still maintained 85.4% of its original response current, indicating a desirable stability.

3.7. Interference determination

Oxidizable compounds such as ascorbic acid and uric acid usually coexist with glucose in real samples and may cause interference on the detection of glucose. The interfering effects of 0.2 mM ascorbic acid, 0.2 mM uric acid and 0.2 mM L-cysteine were examined in the presence of 0.5 mM glucose. As shown in Fig. 7, there was no obvious response after the additions of 0.2 mM ascorbic acid, 0.2 mM uric acid and 0.2 mM L-cysteine to 0.1 M PBS containing 0.5 mM glucose. This result indicates that the proposed glucose biosensor exhibits a high selectivity and good anti-interference ability.

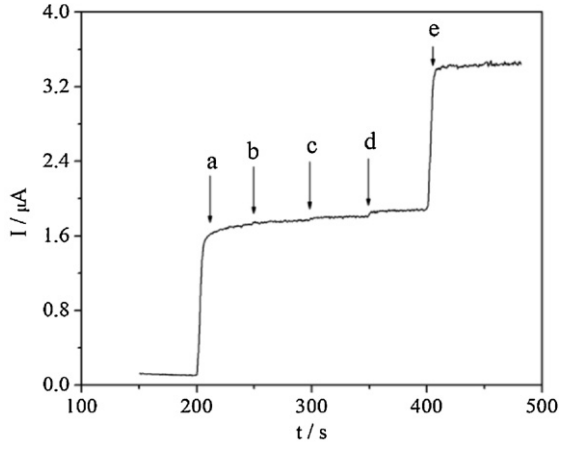

Fig. 7. Amperometric response of the biosensor to (a) 0.5 mM glucose, (b) 0.2 mM ascorbic acid, (c) 0.2 mM uric acid, (d) 0.2 mM L-cysteine and (e) 0.5 mM glucose in 0.1 M PBS at an applied potential of 0.45 V.

Table 2
The recovery of glucose at the biosensor.

Sample	C_{Added} (μM)	$C_{Found} \pm SD^a$ (μM)	RSD (%)	Recovery (%)
1	150	143.6 ± 2.8	1.9	95.7
2	350	358.3 ± 11.1	3.1	102.4
3	550	544.7 ± 12.5	2.3	99.0

[a] Average value from three determinations.

3.8. Recovery experiment

The analytical applicability of the biosensor was evaluated by standard addition method. Table 2 listed the recovery of three samples of different glucose concentrations. The recovery rates were between 95.7% and 102.4%. The satisfying results demonstrate that the biosensor has a great potential for practical application.

4. Conclusions

In the present study, a novel hybrid nanomaterial, Pt–Au@ZnONRs, was prepared through a seed-mediated growth approach on the nanorods. With Pt–Au@ZnONRs and pAu as immobilization matrix, a glucose biosensor was fabricated by biospecific interaction between GOx and lectin (ConA). Owing to the integration of the high electrocatalytic activity of Pt–Au@ZnONRs and the oriented and site-specific immobilization of GOx, the resulted biosensor showed the good performance, such as wide linear range, low detection limit, high sensitivity, low apparent Michaelis–Menten constant (K_M^{app}) and good stability. This construction strategy would offer potential promise for the fabrication of biosensors and biocatalysts.

Acknowledgments

This work is supported by National Natural Science Foundation of China (21075100, 21275119), Municipal Key Laboratory on Luminescence and Real-Time Analysis, Southwest University, and the Fundamental Research Funds for the Central Universities (XDJK2012A004).

References

[1] Wang J. Glucose biosensors: 40 years of advances and challenges. Electroanalysis 2001;13:983–8.
[2] Nakamura H, Karube I. Current research activity in biosensors. Analytical and Bioanalytical Chemistry 2003;377:446–68.
[3] Liu Y, Yu T. Polymers and enzyme biosensors. Journal of Macromolecular Science - Reviews in Macromolecular Chemistry & Physics C 1997;37:459–500.
[4] Lindgren A, Ruzgas T, Gorton L, Csoregi E, Ardila GB, Sakharov IU, Gazaryan IG. Biosensors based on novel peroxidases with improved properties in direct and mediated electron transfer. Biosensors and Bioelectronics 2000;15:491–7.
[5] Netchiporouk LI, Shram NF, Jaffrezic-Renault N, Martelet C, Cespuglio R. In vivo brain glucose measurements: differential normal pulse

voltammetry with enzyme-modified carbon fiber microelectrodes. Analytical Chemistry 1996;68:4358–64.
[6] Doretti L, Ferrara D, Lora S, Palma G. Amperometric biosensor involving covalent immobilization of choline oxidase and butyryl-cholinesterase on a methacrylate-vinylene carbonate co-polymer. Biotechnology and Applied Biochemistry 1999;29:67–72.
[7] Bu HZ, Mikkelsen SR, English AM. NAD(P)H sensors based on enzyme entrapment in ferrocene-containing polyacrylamide-based redox gels. Analytical Chemistry 1998;70:4320–5.
[8] Soto AMG, Jaffari SA, Bone S. Characterisation and optimization of AC conductimetric biosensor. Biosensors and Bioelectronics 2001;16:23–9.
[9] Wu Z, Wang B, Dong S, Wang E. Amperometric glucose biosensor based on lipid film. Biosensors and Bioelectronics 2000;15:143–7.
[10] Butterfield DA, Lee J, Ganapathi S, Bhattacharyya D. Biofunctional membranes IV. Active site structure and stability of an immobilized enzyme, papain, on modified poly-sulfone membranes studies by electron paramagnetic resonance and kinetics. Journal of Membrane Science 1994;91:47–64.
[11] Ganapathi S, Butterfield DA, Bhattacharyya D. Flat-sheet and hollow fibre membrane bioreactors: a study of the kinetics and active site conformational changes of immobilised papain including sorption studies of reaction constituents. Journal of Chemical Technology and Biotechnology 1995;64: 157–64.
[12] Ivanov Y, Marinov I, Gabrovska K, Dimcheva N, Godjevargova T. Amperometric biosensor based on a site-specific immobilization of acetylcholinesterase via affinity bonds on a nanostructured polymer membrane with integrated multiwall carbon nanotubes. Journal of Molecular Catalysis B: Enzymatic 2010;63:141–8.
[13] Anzai J, Kobayashi Y. Construction of multilayer thin films of enzymes by means of sugar–lectin interactions. Langmuir 2000;16:2851–6.
[14] Kobayashi Y, Anzai J. Preparation and optimization of bienzyme multilayer films using lectin and glyco-enzymes for biosensor applications. Journal of Electroanalytical Chemistry 2001;507:250–5.
[15] Li WJ, Yuan R, Chai YQ, Zhong HA, Wang Y. Study of the biosensor based on platinum nanoparticles supported on carbon nanotubes and sugar–lectin biospecific interactions for the determination of glucose. Electrochimica Acta 2011;56:4203–8.
[16] Sun XW, Kwok HS. Optical properties of epitaxially grown zinc oxide films on sapphire by pulsed laser deposition. Journal of Applied Physics 1999;86:408–11.
[17] Ali SMU, Nour O, Willander M, Danielsson B. Glocuse detection with a commercial MOSFET using ZnO nanowires extended gate. IEEE Transaction on Nanotechnology 2009;8:678–83.
[18] Wink T, van Zuilen SJ, Bult A, van Bennekom WP. Self-assembled monolayers for biosensors. Analyst 1997;122:43R–50R.
[19] Ahmad M, Pan CF, Gan L, Nawaz ZS, Zhu J. Highly sensitive amperometric cholesterol biosensor based on Pt-incorporated fullerene-like ZnO Nanospheres. Journal of Physical Chemistry C 2010;114:243–50.
[20] Wang Q, Zheng JB. Electrodeposition of silver nanoparticles on a zinc oxide film: improvement of amperometric sensing sensitivity and stability for hydrogen peroxide determination. Mikrochimica Acta 2010;169: 361–5.
[21] Wang LY, Sun Y, Wang J, Wang J, Yu AM, Zhang HQ, Song DQ. Water-soluble ZnO–Au nanocomposite-based probe for enhanced protein detection in a SPR biosensor system. Journal of Colloid and Interface Science 2010;351: 392–7.
[22] Labib M, Hedström M, Amin M, Mattiasson B. A novel competitive capacitive glucose biosensor based on concanavalin A-labeled nanogold colloids assembled on a polytyramine-modified gold electrode. Analytica Chimica Acta 2010;659:194–200.
[23] Oliveira MDL, Correia MTS, Coelho LCBB, Diniz FB. Electrochemical evaluation of lectin–sugar interaction on gold electrode modified with colloidal gold and polyvinyl butyral. Colloids and Surfaces B 2008;66:13–9.
[24] Zhang XA, Teng YQ, Fu Y, Xu LL, Zhang SP, He B, Wang CG, Zhang W. Lectin-based biosensor strategy for electrochemical assay of glycan expression on living cancer cells. Analytical Chemistry 2010;82:9455–60.
[25] Ragupathy D, Gopalan AI, Lee KP. Synergistic contributions of multiwall carbon nanotubes and gold nanoparticles in a chitosan–ionic liquid matrix towards improved performance for a glucose sensor. Electrochemistry Communications 2009;11:397–401.
[26] Chen H, Xi FN, Gao X, Chen ZC, Lin XF. Bienzyme bionanomultilayer electrode for glucose biosensing based on functional carbon nanotubes and sugar–lectin biospecific interaction. Analytical Biochemistry 2010;403:36–42.
[27] Li CC, Liu YL, Li LM, Du ZF, Xu SJ, Zhang M, Yin XM, Wang TH. A novel amperometric biosensor based on NiO hollow nanospheres for biosensing glucose. Talanta 2008;77:455–9.
[28] Jiang XY, Wu YH, Mao XY, Cui XJ, Zhu LD. Amperometric glucose biosensor based on integration of glucose oxidase with platinum nanoparticles/ordered mesoporous carbon nanocomposite. Sensors and Actuators B 2011;153:158–63.
[29] Wu BY, Hou SH, Yin F, Li J, Zhao ZX, Huang JD, Chen Q. Amperometric glucose biosensor based on layer-by-layer assembly of multilayer films composed of chitosan, gold nanoparticles and glucose oxidase modified Pt electrode. Biosensors and Bioelectronics 2007;22:838–44.
[30] Fu GL, Yue XL, Dai ZF. Glucose biosensor based on covalent immobilization of enzyme in sol–gel composite film combined with Prussian blue/carbon nanotubes hybrid. Biosensors and Bioelectronics 2011;26:3973–6.
[31] Liu JP, Guo CX, Li CM, Li YY, Chi QB, Huang XT, Liao L, Yu T. Carbon-decorated ZnO nanowire array: a novel platform for direct electrochemistry of enzymes and biosensing applications. Electrochemistry Communications 2009;11: 202–5.
[32] Nikoobakht B, El-Sayed MA. Preparation and growth mechanism of gold nanorods (NRs) using seed-mediated growth method. Chemistry of Materials 2003;15:1957–62.
[33] Kamin RA, Wilson GS. Rotating ring-disk enzyme electrode for biocatalysis kinetic studies and characterization of the immobilized enzyme layer. Analytical Chemistry 1980;52:1198–205.